Drug Design, Development and Therapy

Dovepress
open access to scientific and medical research

Open Access Full Text Article

ORIGINAL RESEARCH

Kelussia odoratissima Mozaff. activates intrinsic pathway of apoptosis in breast cancer cells associated with S phase cell cycle arrest via involvement of p21/p27 in vitro and in vivo

This article was published in the following Dove Press journal:
Drug Design, Development and Therapy
1 February 2017
Number of times this article has been viewed

Hamed Karimian[1]
Aditya Arya[2]
Mehran Fadaeinasab[3]
Mahboubeh Razavi[1]
Maryam Hajrezaei[4]
Ataul Karim Khan[1]
Hapipah Mohd Ali[3]
Mahmood Ameen Abdulla[4]
Mohamad Ibrahim Noordin[1,5]

[1]Department of Pharmacy, Faculty of Medicine, University of Malaya, Kuala Lumpur, [2]School of Medicine, Taylor's University, Subang Jaya, [3]Centre for Natural Products Research and Drug Discovery, [4]Department of Biomedical Science, Faculty of Medicine, University of Malaya, Kuala Lumpur, [5]Malaysian Institute of Pharmaceuticals and Nutraceuticals (IPharm), Pulau Pinang, Malaysia

Background: The aim of this study was to evaluate the anticancer potential of *Kelussia odoratissima*. Several in vitro and in vivo biological assays were applied to explore the direct effect of an extract and bioactive compound of this plant against breast cancer cells and its possible mechanism of action.

Materials and methods: *K. odoratissima* methanol extract (KME) was prepared, and MTT assay was used to evaluate the cytotoxicity. To identify the cytotoxic compound, a bioassay-guided investigation was performed on methanol extract. 8-Hydroxy-ar-turmerone was isolated as a bioactive compound. In vivo study was performed in the breast cancer rat model. LA7 cell line was used to induce the breast tumor. Histopathological and expression changes of PCNA, Bcl-2, Bax, p27 and p21 and caspase-3 were examined. The induction of apoptosis was tested using Annexin V-fluorescein isothiocyanate (FITC) assay. To confirm the intrinsic pathway of apoptosis, caspase-7 and caspase-9 assays were utilized. In addition, cell cycle arrest was evaluated.

Results: Our results demonstrated that *K. odoratissima* has an obvious effect on the arrest of proliferation of cancer cells. It induced apoptosis, transduced the cell death signals, decreased the threshold of mitochondrial membrane potential (MMP), upregulated Bax and downregulated Bcl-2.

Conclusion: This study demonstrated that *K. odoratissima* exhibits antitumor activity against breast cancer cells via cell death and cell cycle arrest.

Keywords: *Kelussia odoratissima*, apoptosis, intrinsic pathway, MCF7, chemoprevention, breast cancer

Introduction

Cancer is one of the major health problems of this century.[1] Approximately 12.7 million cancer cases were reported around the world in 2008, and this number is estimated to increase to 21 million by 2030.[2] In general, cancers are slightly more prevalent in men (>6.6 million cases) compared with women (~6.0 million).[3] Breast cancer is one of the most common cancers diagnosed in women, which causes more deaths per year than any other types of cancer.[4] The number of cases diagnosed with breast cancer in Asia has increased steadily over the last several years.[5] In 2006, patients with breast cancer represented 16.5% of all cancer cases reported in Malaysia.[6] Breast cancer is not only the second leading cause of death in Malaysia but also a significant threat to the composition of the society and the national income. In the year 2009, $86.6 billion

Correspondence: Aditya Arya
Clinical and Experimental Pharmacology, School of Medicine, Taylor's University, Lakeside Campus, No 1 Jalan Taylor's, 47500 Subang Jaya, Malaysia
Tel +60 3 5629 5653
Email aditya.arya@taylors.edu.my

Hamed Karimian
Department of Pharmacy, Faculty of Medicine, University of Malaya, 50603 Kuala Lumpur, Malaysia
Tel +60 3 7967 3194
Fax +60 3 7967 4964
Email hamedkarimian61@gmail.com

submit your manuscript | www.dovepress.com
Dovepress
http://dx.doi.org/10.2147/DDDT.S121518

was spent on direct medical costs such as the health expenditures and $130 billion was spent on direct mortality costs, according to the National Institutes of Health (NIH).[7]

Chemotherapy, surgery and radiotherapy are considered as the most common and efficient methods of cancer treatment, although these methods cause severe side effects.[8,9] Gradual resistance of cancer cells against the treatment is considered as one of the biggest problems in cancer therapy, Hence, achieving a new approach to cancer therapy is an important aspect in pharmacological studies to improve the results of cancer treatment. In recent years, plants have played an important role in controlling cancer symptoms and treatments.[10,11] Iran is one of the Asian countries characterized by a diversity of both climate and geographical landscapes. The wide surface area of the country produces >8,000 species of wild plants, and ~700 of these species are classified as medicinal plants.[12] *Kelussia odoratissima* Mozaff. is one of the important plants that belongs to the Umbelliferae family and possesses potential medicinal values. It is solely found in Iran, mainly around the Zagros Mountains at 2,500 m above sea level. This plant is locally called *kelus* or *Karafs-e-Bakhtiari*, and the aerial part of this plant has a high nutritional value due to which natural healers use the plant for its antioxidant, sedative, antiulcerative and anti-inflammatory properties and in the management of cardiovascular disorders.[13–15] In 2015, Behbahani[16] showed that the methanol extracts of flower and leaf and seed extracts of *K. odoratissima* have a potent cytotoxic effect on MCF7 cells. Approximately 27 compounds have been identified from the essential oil of *K. odoratissima*.[17,18] However, due to the few scientific studies on the different parts of this plant, this study was designed to ascertain the potential apoptotic nature of *K. odoratissima* methanol extracts (KMEs) on breast cancer adenoma cells using appropriate mechanisms and correlate the potential in vitro results with in vivo study models.

Materials and methods

Plant materials

K. odoratissima (whole plant) was collected from Shahrekord, Chaharmahal and Bakhtiari, Iran, in February 2012. A voucher specimen (KME-HK) of this plant has been deposited in the Department of Pharmacy, Faculty of Medicine, University of Malaya, as well as in the Herbarium, Biological Institute, Shahrekord Azad University, Iran. The whole plant was dried, weighed and pulverized into powder and stored in a tightly packed glass container at room temperature before further use.

General procedures

Silica gel 60 (40–63 μm; Merck, Darmstadt, Germany) was used to run column chromatography (CC). TLC was completed on glass and aluminum plates, pre-coated with silica gel 60 F_{254} (Merck). Preparative high-performance liquid chromatography (HPLC) was performed with a Waters 2707 instrument (Waters, Milford, MA, USA) with a C-18 Luna column (250 mm×21.2 mm, 5 μm; CA, USA) and PDA 2998 detector (Waters). ^{1}H and ^{13}C 1D NMR and 2D NMR spectra were determined in JEOL JNM-FX500, and the UV spectra were recorded on a Shimadzu UV-160A spectrophotometer using ethanol as the solvent. The MS data were obtained with an Agilent 6530. The IR spectra were measured by Fourier transform IR (FT-IR) spectroscopy using a Perkin-Elmer RX 1 spectrometer for the 4,000–400 cm^{-1} frequency range.

Extraction, purification and isolation methods

Approximately 2.5 kg of *K. odoratissima* powder was extracted at room temperature (Ca. 24°C–27°C) using hexane, chloroform and methanol solvents. The extracts were prepared by soaking 100 g of the coarse powdered plant in 1,000 mL of 95% solvent at room temperature for ~3–4 days. Then, the mixture was filtered, followed by evaporation under low pressure at 45°C using a Buchi-type rotary evaporator to get the dried crude extract. The final yield was calculated as "weight of the crude extract/weight of fresh plant" for every 100 mg plant material. Methanol crude extract of KME was concentrated and eluted through a silica gel column (CH_2Cl_2/MeOH, 100:0 → 50:50), by which four subfractions were obtained. Fraction three was further purified by a preparative HPLC (50%–100% MeOH/H_2O with detection at 252 nm, and a flow rate of 7 mL/min, C18 Column) to yield 8-hydroxy-ar-turmerone (Figure 1).

Cell viability assay

LA7, MCF7, HT29, MDA-MB-231, HepG2, A549, CCD841 and WRL-68 cell lines were purchased from the ATCC (USA). Cell lines were maintained in RPMI 1640 or Dulbecco's Modified Eagle's Medium (DMEM), supplemented with 10% fetal bovine serum (FBS) and 1% penicillin/streptomycin, in a 37°C incubator under 5% of CO_2 saturation. The cell viability assay was determined by an MTT assay. Briefly, cells (1×10^5 cells/cm^2) were treated with all the three crude extracts (hexane, chloroform and methanol extracts) at different concentrations in a 96-well plate, incubated for 24,

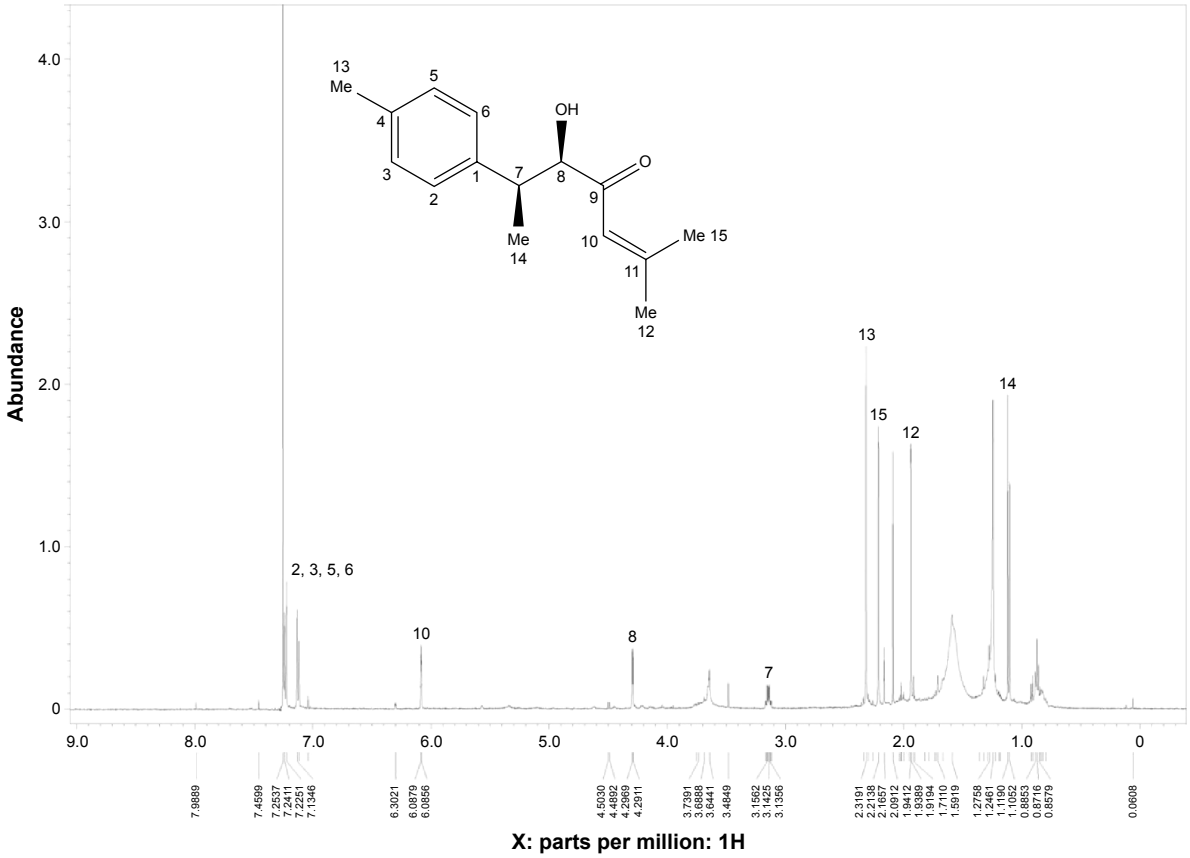

Figure 1 ^{1}H NMR and chemical structures of 8-hydroxy-ar-turmerone.
Abbreviation: NMR, nuclear magnetic resonance.

48 and 72 h, respectively, and then treated with MTT for 3 h and DMSO was added. The colorimetric changes were measured at 570 nm absorbance, and the results were calculated as the percentage of the growth inhibition power.

Animals

A total of 30 female Sprague Dawley® strain rats (180–250 g) were purchased from the animal house facility, Faculty of Medicine, University of Malaya, Malaysia. All the animals were kept in a temperature-controlled room (~24°C) and were supplied with water ad libitum and standard rat pellets. The animal experiment was approved by the ethics committee of the University of Malaya (FAR/26/07/2013HK).

Acute toxicity

Rats weighing an average of 180 g and aged 6–8-week were obtained from the animal house facility, Faculty of Medicine, University of Malaya. The animals were treated with care according to the Guidelines for the Care of Laboratory Animals. A total number of 18 female rats were divided into three different groups placed in three different cages. The first group was fed with Tween 20 10% weight/volume as a vehicle control (VC) group; 5 mL/kg, the second group with LD of KME (2 g/kg) and the third group with the HD of KME (5 g/kg). All the rats were fasted a day before doing the experiment and allowed access to water only. Then, KME was fed to the animals based on the respective dosage and groups, and then they were monitored for 14 days for any signs of toxicity and mortality. Then, the histological parameters were analyzed after sacrificing the animals.[19]

Induction of mammary gland tumors in rats

Tumor development was induced by injecting the rats with LA7 cells. Briefly, the LA7 cells were plated in a culture flask and allowed to reach 90% of confluence. They were then detached using trypsin. The cells were suspended in normal phosphate-buffered saline (PBS) and centrifuged at 580× *g* for 5 min, and 2×10^{6} cells were counted and suspended in 300 µL of PBS. Then, cells were subcutaneously injected into the left flank mammary fat pad of the rats using a tuberculin syringe and 21 G needle.

The mammary tumor development was monitored throughout the experiment. The tumor diameter was measured horizontally and vertically at the end of the experiment. Tumor volume (V) was calculated using the modified ellipsoidal formula: V = (*ab2*)/2, where "*a*" and "*b*" are the longest and shortest diameter of the tumor, respectively. After the experiments, an intraperitoneal injection mixture of xylazine (10 mg/kg body weight) and ketamine HCl (150 mg/kg body weight) was used to anesthetize the animals.[19,20]

Histopathology

The breast tumors were excised from the rats and fixed in 10% formalin. The fixed tissues were processed in a paraffin tissue-processing machine (Leica Microsystems Inc., Nussloch, Germany), and the paraffin blocks were cut into 5 µm sections and stained with hematoxylin and eosin (H&E) dye and periodic acid–Schiff (PAS) dye (Sigma-Aldrich). The morphology of breast tumor tissue was evaluated by observing the sections under a light microscope (Nikon, Tokyo, Japan).

TUNEL assay

Apoptotic cells were captured by combining flourescein-12-dUTP(a) at 3′-OH DNA ends via the terminal recombinant deoxynucleotidyl transferase enzyme (rTdT). The tumor tissue sections were subjected to a DeadEnd™ Fluorometric TUNEL system (Promega Corporation, Madison, WI, USA), according to the manufacturer's instructions, and then captured using a confocal microscope (Zeiss, LSM 70) using standard fluorescein filters.[19]

Immunohistochemistry

Expressions of PCNA, Bax, Bcl-2, p53, p21 and p21 were evaluated using immunohistochemistry analysis. Briefly, after processing the tumor tissues, the sections were incubated with primary antibodies against PCNA, Bcl-2, Bax, p53, p21 and p27 (Santa Cruz Biotechnology). After washing, the sections were incubated with a biotinylated secondary antibody. The sections were evaluated using a DAB Detection Kit (Dako, Glostrup, Denmark). A microscope (BX51; Olympus, Tokoyo, Japan) was used to capture the images of the sections.

Annexin V-FITC assay

Early and late apoptosis induction in MCF7 cells was further examined via the Annexin V-FITC staining assay. Briefly, breast cancer cells (1×10^5) were seeded into a chamber slide, treated with an IC_{50} of 8-hydroxy-ar-turmerone, washed with PBS, and resuspended in a staining solution of Annexin V-FITC according to the manufacturer's protocol. The cells were examined under a fluorescence microscope (Olympus BX51).[21]

Caspase analysis

Commercial kits (Caspase-Glo®-7 assay and Caspase-Glo®-9 assay: Promega Corporation) were purchased. A total of 20,000 MCF7 cells/well were plated into a white 96-well plate and incubated overnight. The cells were then treated with IC_{50} of 8-hydroxy-ar-turmerone for 3, 6, 12, 24 and 48 h. After incubation with 8-hydroxy-ar-turmerone, the plates were kept at room temperature, and then 50 µL of Caspase-Glo® Reagent (7 and 9) was added to the wells. The cells were then incubated at room temperature on a plate shaker for 20 min. Luminescent intensity was quantified using a luminescence microplate reader (Infinite M200PRO; Tecan, Männedorf, Switzerland).

Cell cycle analysis

After treatment, MCF7 cells were spun down at 580× *g* for 5 min, the supernatant was discarded and the remaining pellet was washed with PBS. The cell pellets were then fixed with 700 µL of 90% cold ethanol at 4°C overnight. After fixing, the cells were spun down at 200× *g* for 5 min, the ethanol was discarded and the cells were resuspended in 600 µL of PBS. Approximately 25 µL of RNaseA (10 mg/mL) mixed with 50 µL of propidium iodide (PI; 1 mg/mL) was added to the cells at 37°C for ~1 h. PI is capable of binding the RNA molecules; therefore, RNase enzymes were added, to allow for direct binding of PI to the DNA, and the fluorescence was measured by the flow cytometer (BD FACSCanto™ II).[22,23]

Statistical analysis

Counts from different treatment groups were calculated from different observational fields and analyzed for each experiment (n). Each experiment was performed in triplicate and repeated at least three times. The recorded data were fed into a computer program (Window XP, Excel). One-way ANOVA (Dunnett's multiple comparison test) was used for independent samples followed by Tukey's post hoc test using SPSS-17.0 (IBM Corporation, New York, NY, USA) and GraphPad prism (version 4.0; Graphpad Software Inc, La Jolla, CA, USA). A *P*-value of <0.05 was considered significant, and all the values were reported as mean ± SD.

Results

Chemical elucidation of the isolated compound

8-Hydroxy-ar-turmerone was isolated as a white oil with an optical rotation of $[\alpha]_D^{24} -62$ (*c* 0.05, $CHCl_3$). The high-resolution electrospray ionization mass spectrometry (HRES-IMS) showed a molecular ion at *m/z* 233.1562 (M + H) + (calcd for $C_{15}H_{20}O_2$). The ultraviolet (UV) spectrum exposed maxima at 230 nm. In addition, the infrared (IR) ($CHCl_3$) spectrum showed peaks at 1,691 cm^{-1} (carbonyl ketone group stretching) and 3,351 cm^{-1}, which indicated the presence of an OH group. The ^1H nuclear magnetic resonance (NMR) spectrum showed the existence of two overlapped aromatic signals at δ 7.13 (2H, *dd*, *J* =1.3, 7.2 Hz) and δ 7.25 (2H, *dd*, *J* =1.3, 7.2 Hz) due to protons on C-3, C-6, C-2 and C-5, respectively (Figure 1). A peak at δ6.08 *d* (1.1) was assigned to H-10. Another two peaks appeared at δ3.14 *m* and 4.29 *d* (2.9), which was attributed to protons of two methines linked to C-7 and C-8, respectively. Four peaks at δ1.93 *s*, 2.3 *s*, 1.11 *d* (6.9) and 2.21 were assigned to four methyl groups. The ^{13}C NMR spectrum of 8-hydroxy-ar-turmerone specified the existence of 15 carbons, counting with five quaternary carbons, six methines and four methyl groups based on the DEPT spectrum (Table 1).

Cytotoxic activity

The MTT assay was performed to determine the level of cell viability and the degree of cytotoxicity produced by the addition of all three extracts to the cells. MCF7 was found to be the most sensitive cells to KME (Figure 2). The positive control (tamoxifen; Sigma-Aldrich) was used as the positive control with half maximal inhibitory concentration (IC_{50}) value lower than KME. Dimethyl sulfoxide (DMSO) at a concentration of 0.1% was used as a vehicle control, and the results did not show any sign of toxicity. Moreover, an in vivo study was performed on the KME, whereas the in vitro study was accomplished with 8-hydroxy-ar-turmerone as a bioactive compound (Table 2).

Acute toxicity

The results of the acute toxicity study revealed the nontoxic nature of the plant even at the higher dose tested. During the 14-day monitoring, no signs of mortality were observed and the slides of the kidney and liver confirmed the safety of KME.

Size and volume of the tumor

The appearance of the tumor was observed during the early 10 days after the injection of LA7 cells to the rats. Tumor size, percentage and body weights of the animals are presented in Table 3. No significant decrease in body weight was observed in the control and treatment group animals. However, the tumor size was significantly reduced in the KME- and tamoxifen-treated groups (Figure 3).

Histopathology

The histopathological observation of the slides from non-neoplastic breast of the rats showed lactiferous ducts and acini with some vessels and stroma. After tumor induction, there was a neoplastic proliferation of epithelial cells with severe pleomorphism and mitotic activity. The treatment

Table 1 ^1H NMR (500 MHz) and ^{13}C NMR (125 MHz) spectral data of 8-hydroxy-ar-turmerone in $CDCl_3$ (δ in ppm, *J* in Hz)

Position	^1H NMR (δ ppm)	^{13}C NMR (δ ppm)
1	–	140.8
2	7.25 *dd* (7.2, 1.3)	129.1
3	7.13 *dd* (7.2, 1.3)	129.1
4	–	136.2
5	7.25 *dd* (7.2, 1.3)	127.6
6	7.13 *dd* (7.2, 1.3)	127.6
7	3.14 *m*	42.3
8	4.29 *d* (2.9)	80.5
9	–	200.2
10	6.08 *d* (1.1)	119.8
11	–	159.5
12	1.93 *s*	29.7
13	2.3 *s*	21.5
14	1.11 *d* (6.9)	13.9
15	2.21 *s*	28.1

Abbreviation: NMR, nuclear magnetic resonance.

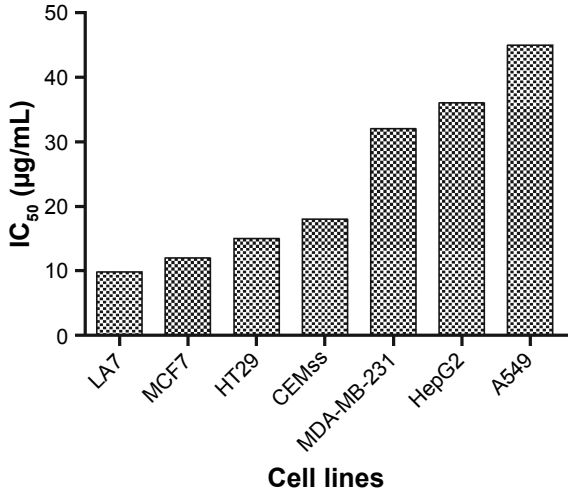

Figure 2 Cytotoxicity effect of KME against different cell lines.
Abbreviations: IC_{50}, half maximal inhibitory concentration; KME, *Kelussia odoratissima* methanol extract.

Table 2 KME and 8-hydroxy-ar-turmerone were tested against MCF7, LA7 and MCF10A cell lines

Cell lines	Compounds								
	8-hydroxy-ar-turmerone (24 h)	Tamoxifen (24 h)	KME (24 h)	8-hydroxy-ar-turmerone (48 h)	Tamoxifen (48 h)	KME (48 h)	8-hydroxy-ar-turmerone (72 h)	Tamoxifen (72 h)	KME (72 h)
MCF7 (μg/mL)	12.41±0.81	7.38±0.18	19.72±1.49	6.52±0.27	3.19±0.36	11.97±1.82	4.31±0.53	1.6±0.19	7.25±0.34
LA7 (μg/mL)	10.18±1.71	8.59±0.14	16.37±0.24	6.81±0.72	3.11±0.57	9.87±1.69	5.04±0.65	2.18±0.26	6.91±0.97
MCF10A (μg/mL)	86.91±2.16	72.38±1.72	100	72.17±3.73	65.91±2.44	100	66.15±1.76	44.83±2.37	100

Notes: The viability of the cells was determined by an MTT assay. The test agent induced cell cytotoxicity in a time-dependent manner. Dose titration curves were used to determine the IC_{50} of the test agent toward these cell lines.
Abbreviations: IC_{50}, half maximal inhibitory concentration; KME, *Kelussia odoratissima* methanol extract.

demonstrated wide areas of necrosis, apoptosis and regression of tumor. In spite of having many changes in the breast tissue, the hepatic and renal tissues had normal histology, including hepatic lobules, renal ducts and glomeruli without any evidence of toxicity or fibrosis (Figure 4).

TUNEL assay

The TUNEL assay was performed to confirm the induction of apoptosis in the treatment groups. Apoptotic cells are illustrated by the fluorescence green color of the free labeled 3′-OH termini. The result demonstrated that several cells had undergone apoptosis at the high dose (HD) in the KME- and tamoxifen-treated groups, whereas no noticeable numbers of apoptotic cells were witnessed in the low-dose (LD) and control groups (Figure 5).

Immunohistochemistry

Immunohistochemistry analysis of the tumor sections revealed that the expression of the tumor markers PCNA and Ki-67 increased in the cancer control group. However, in the treatment groups, these tumor markers were significantly decreased and disappeared (Figure 6).

The tumor apoptosis markers Bax, Bcl-2, caspase-3 and p53 were found to exhibit an upregulation trend in the treatment groups, while there was no expression in the cancer control group. Interestingly, Bcl-2 was highly expressed in the cancer control group, where it was decreased in the treatment groups (Figure 7). The cell cycle markers p21 and p27 were remarkably expressed in the treated groups, while there was negligible expression in the cancer control group (Figure 8).

In vitro examination of 8-hydroxy-ar-turmerone against MCF7 cells

Annexin V-fluorescein isothiocyanate (FITC) assay

Induction of early apoptosis was confirmed by phosphatidylserine externalization in 8-hydroxy-ar-turmerone-treated cells. Microscopic observations confirmed the morphological and cellular adjustment under 48 h of treatment as shown in Figure 9. The MCF7 cells exhibited remarkable blebbing from the cell membrane with positive expression of Annexin V (Figure 9).[24]

Analysis of caspase-9 and caspase-7

Caspase-9 significantly increased after treatment of MCF7 cells with 8-hydroxy-ar-turmerone at 12 h, while caspase-7 remarkably increased at 24 and 48 h after 8-hydroxy-ar-turmerone treatment ($P<0.05$; Figure 10).

Table 3 Reduction in tumor size in the high dose KME and tamoxifen-treated groups

Group	Treatment groups	Body weight (g)	Tumor volume (mm^3)	Reduction in tumor (%)
I	NC	292.9±15.68	0	0
II	TC	278.37±13.49	2,024±252	0
III	TT + LD	288.17±6.82	1,873±194	7.46
IV	TT + HD	274.39±14.62	521±86*	74.25*
V	TT + TAM	232.54±18.79	363±108*	82.06*

Notes: Data are shown as mean ± SEM. Values are statistically significant at *$P<0.05$.
Abbreviations: HD, high dose; KME, *Kelussia odoratissima* methanol extract; LD, low dose; NC, normal control; SEM, standard error of the mean; TC, tumor control; TT + HD, tumor treated with HD KME; TT + LD, tumor treated with LD KME; TT + TAM, tumor treated with tamoxifen.

Cell cycle arrest

Cell cycle disruption was observed in correlation to the cell cycle phase distributions (G_0, G_1, S, G_2 and M). This result shows that 8-hydroxy-ar-turmerone arrested cell proliferation at the S cycle phase in a time-dependent manner at 24, 48 and 72 h of 8-hydroxy-ar-turmerone treatment. Specifically, the G_0/G_1 phase and G_2/M phase were reduced at higher concentrations of 8-hydroxy-ar-turmerone (Figure 11; $P<0.05$).

Discussion

Usage of herbal drugs and medicinal plants for their active compounds has been increasing globally for the management of inflammatory responses and certain cancers.[25] *K. odoratissima* is one of the culinary plants, which is widely consumed by the people of Iran to keep certain cancers away with its daily use; however, not much effort has been made to study the biologically active compounds of this plant against cancer.[14,26]

KME was investigated for its anticancer potential and possible mechanism against cancer cells. Our study results demonstrated the cytotoxic effect of KME against various cancer cells, including MCF7, LA7, HT29, CEMss, MDA-MB-231, HepG2 and A549. However, MCF7 breast cancer adenoma cells showed the lowest IC_{50} with remarkable decrease in the cell population and viability according to the cell cycle arrest; thus, we determined the effects of KME in an animal breast cancer model, and subsequently bioassay-guided assays were performed with 8-hydroxy-ar-turmerone as a bioactive compound in KME. The structure of 8-hydroxy-ar-turmerone was confirmed by 2D NMR spectroscopy, and the presence of carbonyl group at C-9 was demonstrated via a correlation between the carbonyl signal δ 200.2 and the signal due to H-10 at δ 6.08 in the heteronuclear multiple-bond correlation (HMBC) spectrum. The HMBC spectrum also showed correlations between the signals from H-7 to C-6, H-12 to C-11 and H-14 to C-8.

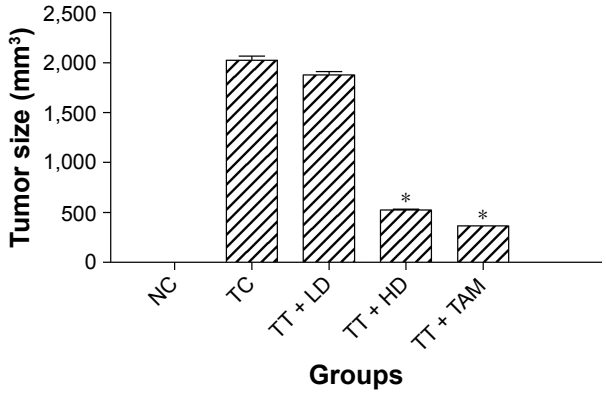

Figure 3 Breast cancer tumor volume in different groups.
Notes: Tumor size was significantly reduced in the HD KME- and tamoxifen-treated groups. Data are shown as mean ± SEM. Values are statistically significant at *$P<0.05$.
Abbreviations: HD, high dose; KME, *Kelussia odoratissima* methanol extract; LD, low dose; NC, normal control; SEM, standard error of the mean; TC, tumor control; TT + HD, tumor treated with HD KME; TT + LD, tumor treated with LD KME; TT + TAM, tumor treated with tamoxifen.

The results of the acute toxicity study show the nontoxic nature of KME, and the microscopic observation illustrates the glomeruli without signs of toxicity or fibrosis with normal hepatic lobules and renal ducts. These outcomes are in line with the usage of this plant by the Iranians for edible purpose; furthermore, oral treatments of HD KME and tamoxifen to the LA7-induced breast cancer groups indicated the suppression of smaller sized tumors compared with the control group. In addition, these results were established by histopathological examination of the tumor sections, which showed the presence of invasive breast tumor in which the ductal morphology of the cancer-induced groups was completely changed and disappeared in most of the breast tissues after KME treatment.

Furthermore, it is well known that PCNA and Ki-67 are the most commonly used proliferative markers for identifying the presence of breast cancer in breast tissues. Interestingly, in the current study, we observed that PCNA and Ki-67 were clearly increased after tumor development as indicated by the immunohistochemistry analysis. Despite the high number of cancer cells in the cancer control group, the number of

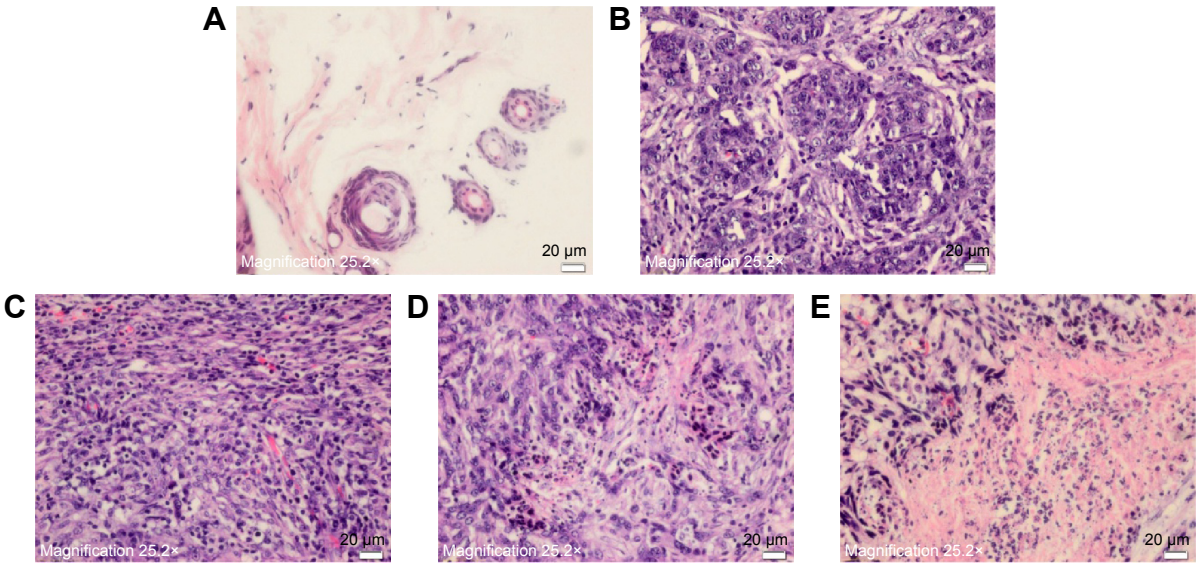

Figure 4 Histological examination of breast cancer tissue.
Notes: (**A**) Normal breast tissue. (**B**) Tumor control. (**C**) LD KME treatment. (**D**) HD KME treatment. (**E**) Tamoxifen treatment. Histological study of the breast sections shows the morphology changes of the breast tissues. Magnification, 25.2×.
Abbreviations: HD, high dose; KME, *Kelussia odoratissima* methanol extract; LD, low dose.

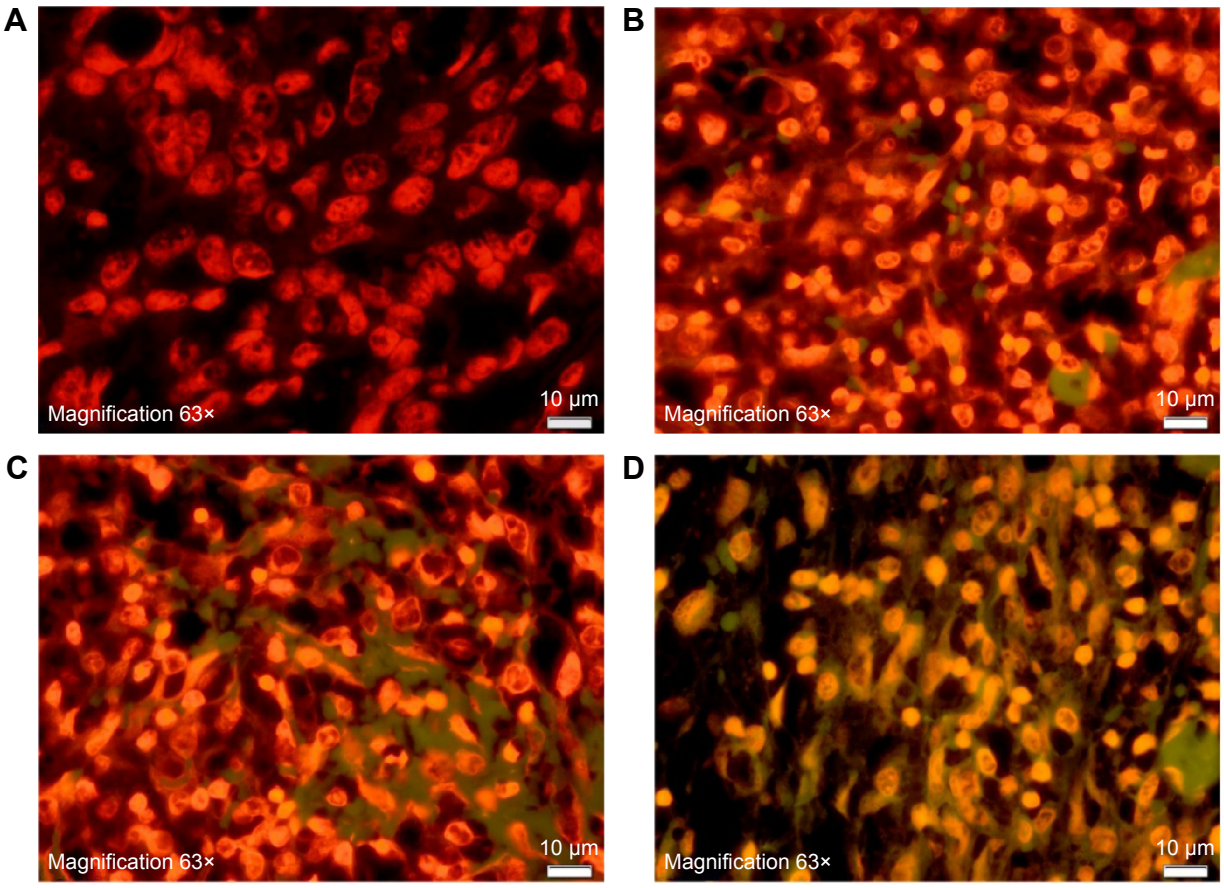

Figure 5 Apoptosis confirmation using the TUNEL assay.
Notes: (**A**) Tumor control. (**B**) LD KME treatment. (**C**) HD KME treatment. (**D**) Tamoxifen treatment. Tumor sections were subjected to TUNEL assay. The HD KME- and tamoxifen-treated groups showed remarkable numbers of apoptotic cells compared with the tumor control group. Magnification, 63×.
Abbreviations: HD, high dose; KME, *Kelussia odoratissima* methanol extract; LD, low dose.

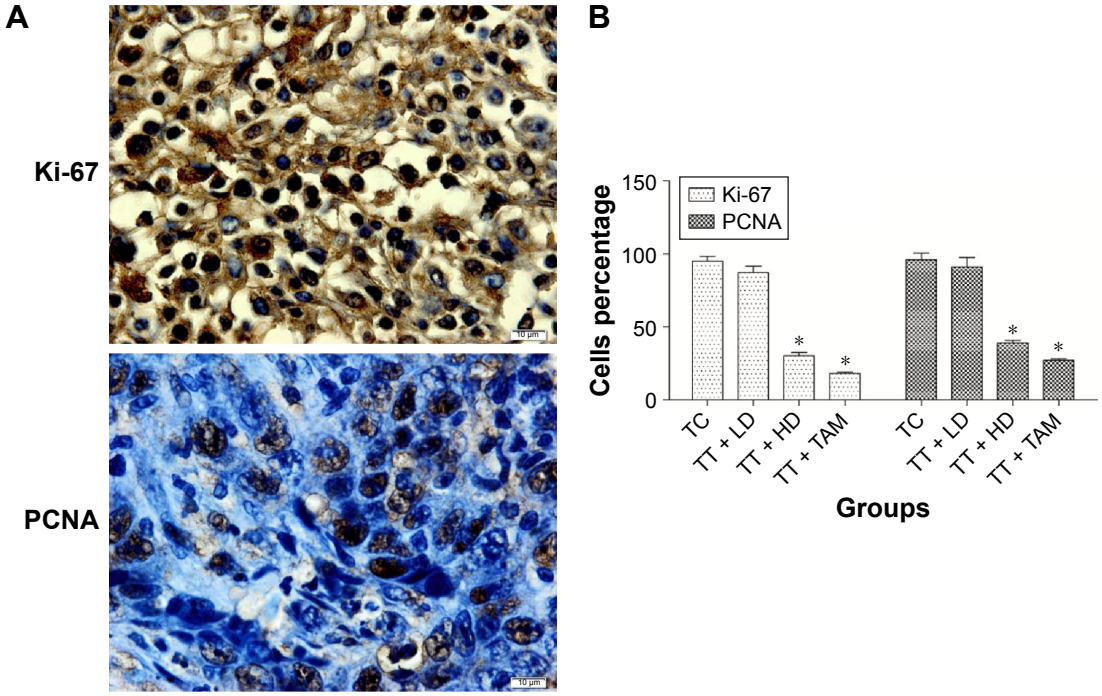

Figure 6 Immunohistochemical analysis of tumor proliferation markers.
Notes: Ki-67 and PCNA are tumor markers, and brown particles with irregular shapes indicate PCNA and Ki-67 expression (**A**), LD and HD KME- and tamoxifen-treated groups (**B**). Ki-67 and PCNA quantification represents the significant reduction in tumor cells after treatment with HD KME and tamoxifen (**B**). Data are shown as mean ± SEM. Values are statistically significant at $^*P<0.05$. Magnification, 100×.
Abbreviations: HD, high dose; KME, *Kelussia odoratissima* methanol extract; LD, low dose; SEM, standard error of the mean; TC, tumor control; TT + HD, tumor treated with HD KME; TT + LD, tumor treated with LD KME; TT + TAM, tumor treated with tamoxifen.

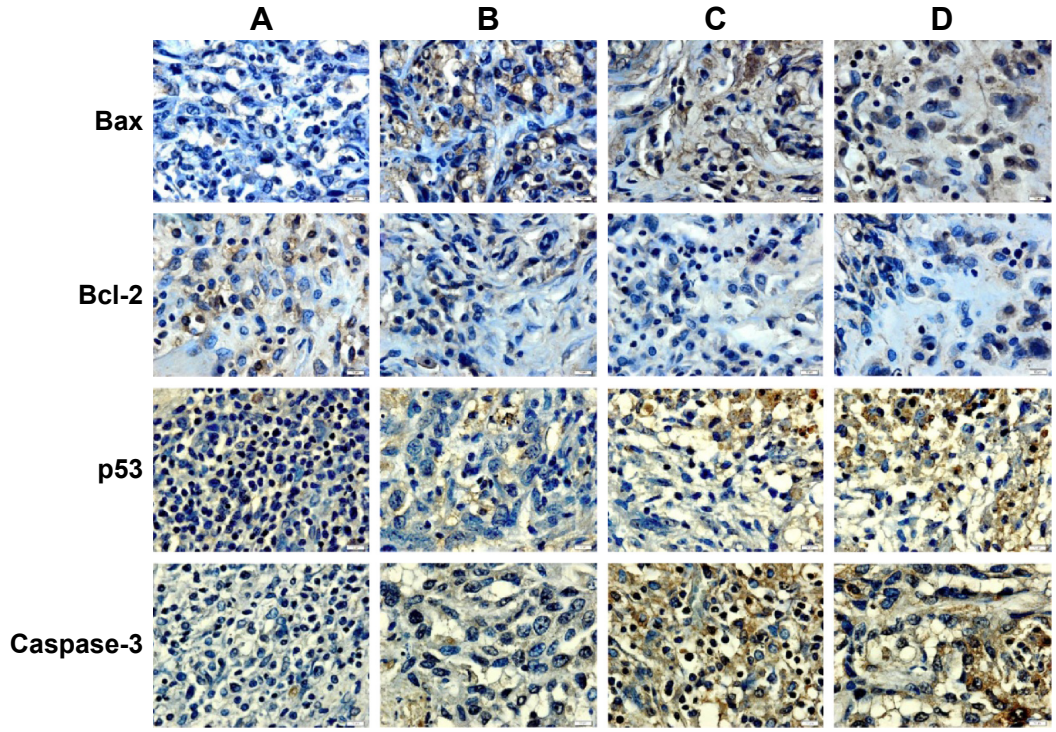

Figure 7 Immunohistochemical results of apoptotic markers.
Notes: Tumor control (**A**), LD KME treatment (**B**), HD KME treatment (**C**) and tamoxifen treatment (**D**). Brown particles represent Bax, Bcl-2, p53 and caspase-3 protein expression. Microscopic observation illustrates the high expression of Bax, p53 and caspase-3 and a low expression of Bcl-2 in the HD KME- and tamoxifen-treated groups. Magnification, 100×.
Abbreviations: HD, high dose; KME, *Kelussia odoratissima* methanol extract; LD, low dose.

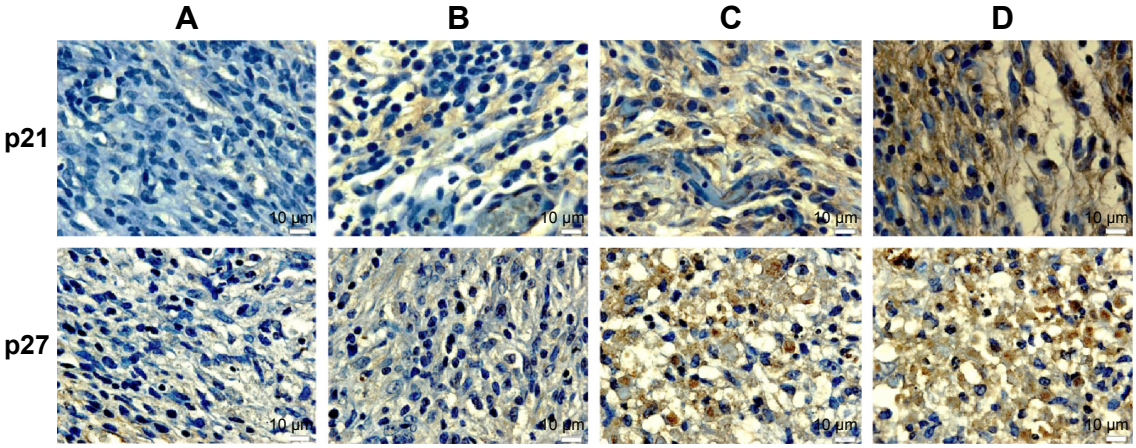

Figure 8 Immunohistochemical study of cell cycle markers.
Notes: Tumor control (**A**), LD KME treatment (**B**), HD KME treatment (**C**) and tamoxifen treatment (**D**). The brown particles represent the p21 and p27 protein expression. HD KME- and tamoxifen-treated groups highlight the expression of p21 and p27 after treatment, which confirms the cell cycle arrest. Magnification, 100×.
Abbreviations: HD, high dose; KME, *Kelussia odoratissima* methanol extract; LD, low dose.

positive cancer cells was remarkably reduced after KME and tamoxifen treatments.

Moreover, in line with the microscopic and morphological outcomes of our findings supporting the beneficial effects of KME in suppressing the tumor cells, the underlying mechanism can be attributed to apoptosis based on the confirmation of the induction of apoptosis by KME and compound treatments. In the TUNEL assay, the fragmented DNA in apoptotic cells can combine with the flourescein-12-dUTP(a) that produces the green fluorescence dye, which illustrates

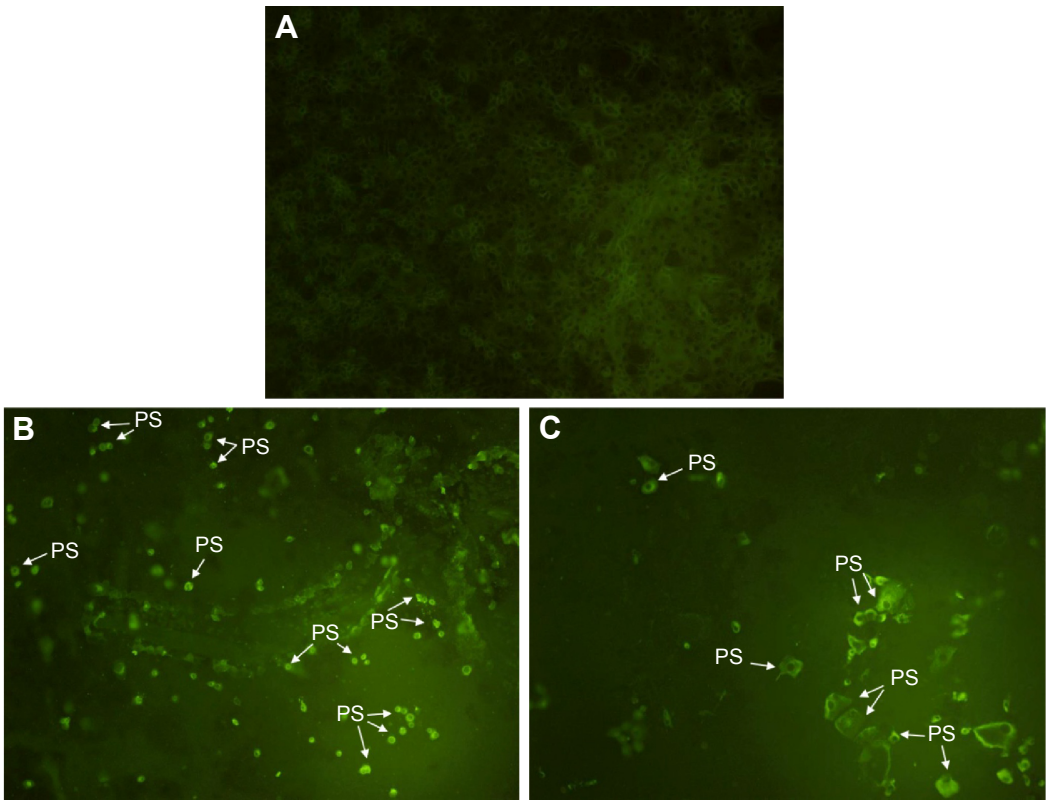

Figure 9 Early apoptosis validation.
Notes: MCF7 cells were treated with IC_{50} of 8-hydroxy-ar-turmerone for 48 h. Cells were incubated for 20 min with Annexin V-FITC and the buffer. Untreated cells showed viable cells with no signs of apoptosis (**A**). Light green stained with Annexin V-FITC revealed that PS residues had been translocated to the membrane and externalized (phosphatidylserine) after treatment. Treated cells are shown with (**B**) 20× and (**C**) 40× magnification.
Abbreviations: FITC, fluorescein isothiocyanate; IC_{50}, half maximal inhibitory concentration.

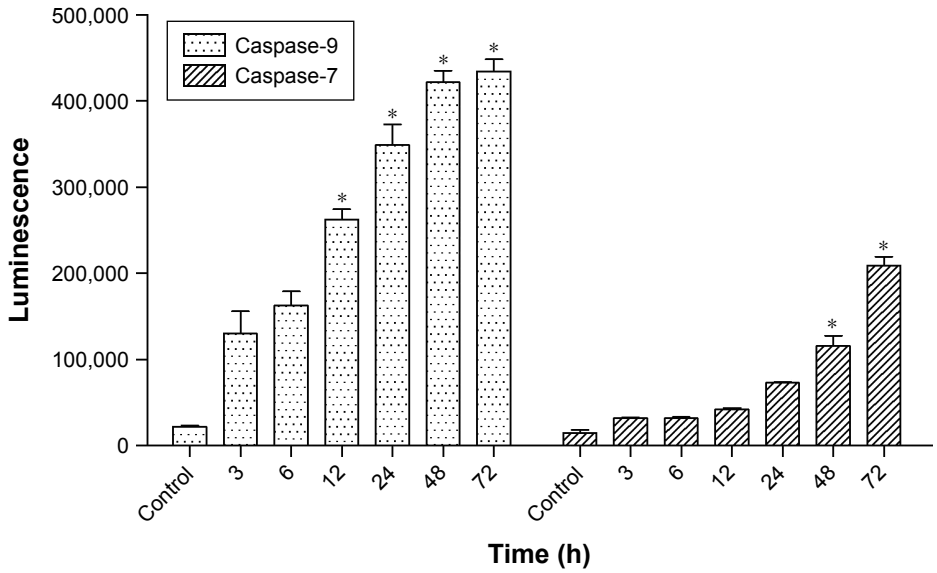

Figure 10 Caspase-9 and caspase-7 luminescence evaluation in MCF7 cells during 8-hydroxy-ar-turmerone treatment.
Notes: Data represent a remarkable increase in caspase-9 after 12 h and caspase-7 in 72 h. This confirmed the activation of the intrinsic pathway of apoptosis after 8-hydroxy-ar-turmerone treatment. Data are shown as mean ± SD (n=3). *A significant difference ($P<0.05$) compared with the control.

the induction of apoptosis in the cells, where HD KME and tamoxifen treatment of the tumor sections confirmed the presence of apoptotic cells. Similarly, the cellular membrane leakage and increase in permeability caused internalization of PS protein, following translocation of the protein from the inner surface to the outer surface of the plasma membrane, and induced Annexin V redistribution from vesicles to the apical pole of the membrane. In turn, all the cells treated with 8-hydroxy-ar-turmerone showed a significant induction of Annexin V response with positive fluorescence expression. As such, our data reveal that 8-hydroxy-ar-turmerone can activate the intrinsic functional membrane in MCF7 cells, thereby causing apoptosis.[27,28]

The commitment of cells to undergo programmed suicide or apoptosis, which is determined by the Bcl-2 family proteins, is crucial for tissue homeostasis, development and immunity. Apoptosis is activated in mammals through an intrinsic pathway, which involves the mitochondria or death receptors in the extrinsic pathway. Mitochondria are regulated in apoptosis through the members of Bcl-2 family proteins. Bcl-2 proteins are either proapoptotic or antiapoptotic and regulate the intrinsic pathway of apoptosis through the mitochondrial membrane.

All intracellularly retained cytochrome *c*, Bax and Bcl-2 are considered as early mediators of apoptosis; they are, in fact, localized to a great extent in the late apoptotic pathway.[29,30] A paradigm is that mitochondrial integral membrane protein domains exchange on their way to the cytosol through the mitochondrial membrane potential (MMP), mainly by passing through the mitochondrial membrane transition pores (MPTPs). Our in vitro and in vivo analyses revealed that cancer cells stably express Bax functional protein regardless of the treatments.[22,31] The upregulation of Bax and the downregulation of Bcl-2 were equally sensitive to both KME and 8-hydroxy-ar-turmerone as well as to tamoxifen. The regulation of the apoptotic modulators was further supported by p53 with KME treatments. The low numbers of cancer cell population bypassing the G_0/G_1 and G_2/M phases may directly be delivered by post-apoptotic processing via the conventional cytokines.[32]

Caspases have been identified as components of the cellular apoptotic complex. They have also been proposed to have a role in mitochondrial integrity and may serve as initiators for intrinsic/extrinsic succession involved in various cellular processes.[33] Cellular processes, which are essential for nuclear functionality and stability, are maintained by a series of caspases, accompanied with specific enzymatic events. Caspases share some features of both apoptosis and mitosis signaling as well as cytoskeletal protein domains, ie, Bax and Bcl-2.[34] Therefore, studying the functions of caspases as positive regulators of apoptotic cascade is of utmost interest. Our data indicate an appreciable shift of caspase-9 and caspase-7 expressions by 8-hydroxy-ar-turmerone in MCF7 cells. 8-Hydroxy-ar-turmerone clearly acted at the mitochondrial level and increased the expression of caspases in a time-dependent manner, unlike in the untreated cells where the levels of caspase-9 and caspase-7 expressions were unaffected. Caspase-9 activation was initiated at an earlier

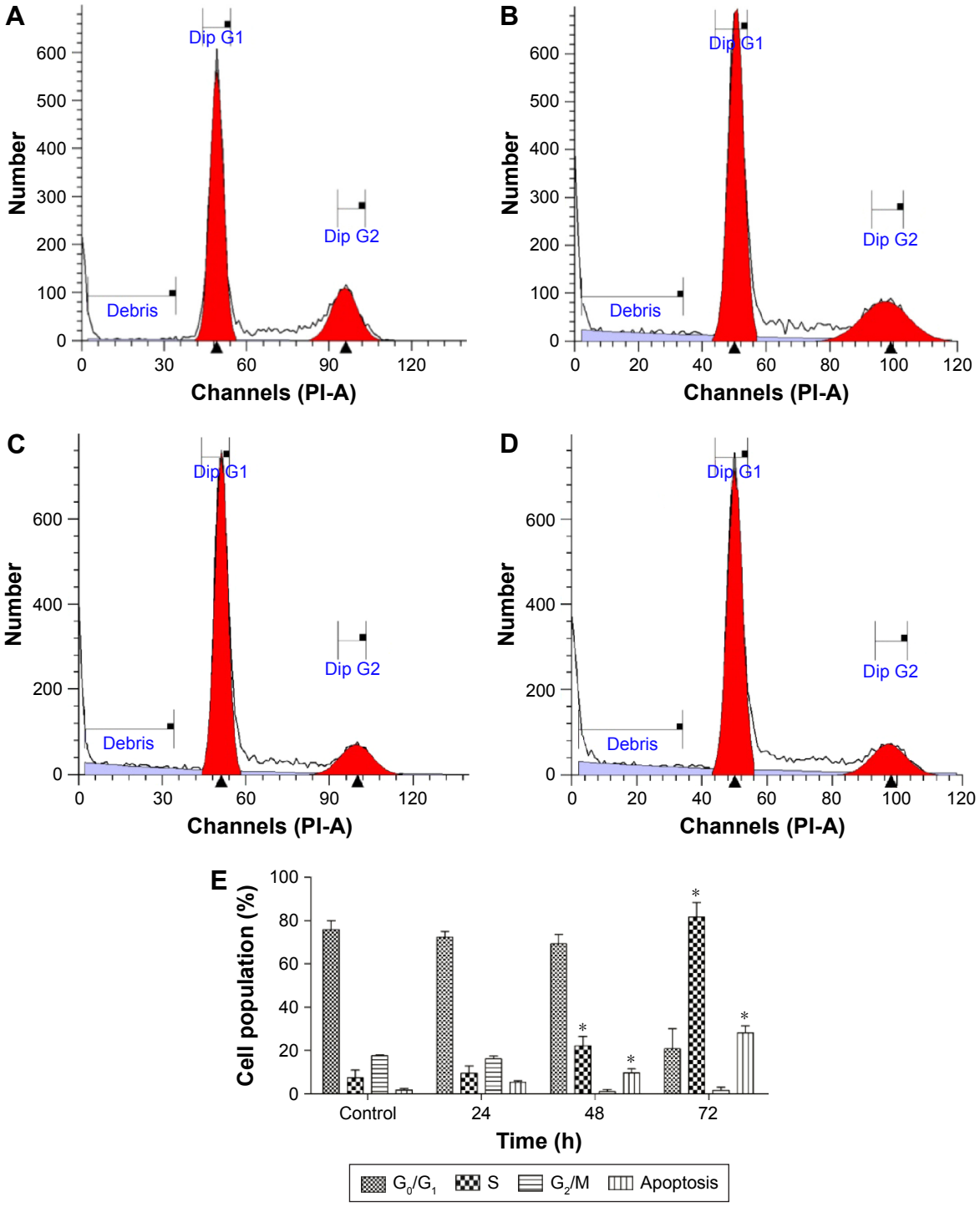

Figure 11 Flow cytometric analysis of cell cycle distribution in MCF7 cell line.
Notes: Cells were treated with IC_{50} of 8-hydroxy-ar-turmerone for 24, 48 and 72 h. The histogram is represented as: (**A**) control; (**B**) 24 h; (**C**) 48 h and (**D**) 74 h. Cells were cultured in RPMI 1640 (25 mL flask) media maintained at 37°C and 5% CO_2. (**E**) Data represents the significant elevation of the cells numbers in S phase after 48 and 72 hours of treatment. Data are shown as mean ± SD (n=3). *Significant difference ($P<0.05$) compared with the control.
Abbreviations: IC_{50}, half maximal inhibitory concentration; PI-A, propidium iodide A channel.

phase causing an activation of the caspase cascade involved in the intrinsic pathway. The activation of caspase-9 was clearly organized with the help of the apoptosome, where procaspase-9 was converted to caspase-9. This is most likely due to the involvement of the intrinsic pathway. Accordingly, KME-treated sections were analyzed through the expression of the executioner caspase-7, which revealed the activation of caspase-7 in the tumor sections after KME treatment.[35–37]

Moreover, the in vitro results regarding the expression of p21 and p27 proteins with 8-hydroxy-ar-turmerone treatments were further studied on MCF7 cells to determine the possible characteristics of arrest. Our findings are in line with the cyclin-dependent kinase inhibitors that regulate the proliferation of cells in association with other proteins. The upregulation of these proteins can stop the proliferation of the cells as indicated by our results, which show the upregulation of p21 and p27 after treatment with 8-hydroxy-ar-turmerone and KME in vitro and in vivo, respectively, while there was no significant expression in the cancer control group.

Conclusion

Overall, our study results revealed that *K. odoratissima* has potential anticancer effects against breast cancer cells in vitro and in vivo. Our data proposed that KME can initiate antiproliferative and apoptotic effects and destroy the tumor cells by disrupting the cell membrane and dysfunctioning the mitochondrial metabolic cascade, as well as disrupting the expression of Bax and Bcl-2 via the intrinsic pathway. 8-Hydroxy-ar-turmerone is identified as the active compound that contributes best to the anticancer activity.

Acknowledgments

All the data generated or analyzed during this study are included in this article. This research work is supported by the fundamental research grant (FRGS): FP021-2014A from the ministry of higher education, and RP043B-15HTM Malaysia.

Disclosure

The authors report no conflicts of interest in this work.

References

1. Kanavos P. The rising burden of cancer in the developing world. *Ann Oncol*. 2006;17(suppl 8):viii15–viii23.
2. Bray F, Jemal A, Grey N, Ferlay J, Forman D. Global cancer transitions according to the human development index (2008–2030): a population-based study. *Lancet Oncol*. 2012;13(8):790–801.
3. Greenlee RT, Hill-Harmon MB, Murray T, Thun M. Cancer statistics, 2001. *CA Cancer J Clin*. 2001;51(1):15–36.
4. DeSantis C, Siegel R, Bandi P, Jemal A. Breast cancer statistics, 2011. *CA Cancer J Clin*. 2011;61(6):408–418.
5. Deapen D, Liu L, Perkins C, Bernstein L, Ross RK. Rapidly rising breast cancer incidence rates among Asian–American women. *Int J Cancer*. 2002;99(5):747–750.
6. Lin Y, Shao N, Zhang YJ, et al. Risk assessment of breast cancer in Guangdong, China: a community-based survey. *Asian Pac J Cancer Prev*. 2012;13(6):2759–2763.
7. Mariotto AB, Yabroff KR, Shao Y, Feuer EJ, Brown ML. Projections of the cost of cancer care in the United States: 2010–2020. *J Natl Cancer Inst*. 2011;103(2):117–128.
8. Bower JE, Ganz PA, Desmond KA, Rowland JH, Meyerowitz BE, Belin TR. Fatigue in breast cancer survivors: occurrence, correlates, and impact on quality of life. *J Clin Oncol*. 2000;18(4):743–743.
9. Sun S-Y, Hail N, Lotan R. Apoptosis as a novel target for cancer chemoprevention. *J Natl Cancer Inst*. 2004;96(9):662–672.
10. Safarzadeh E, Sandoghchian Shotorbani S, Baradaran B. Herbal medicine as inducers of apoptosis in cancer treatment. *Adv Pharm Bull*. 2014;4(suppl 1):421–427.
11. Wartenberg M, Budde P, de Mareés M, et al. Inhibition of tumor-induced angiogenesis and matrix-metalloproteinase expression in confrontation cultures of embryoid bodies and tumor spheroids by plant ingredients used in traditional Chinese medicine. *Lab Invest*. 2003;83(1):87–98.
12. Miraldi E, Ferri S, Mostaghimi V. Botanical drugs and preparations in the traditional medicine of West Azerbaijan (Iran). *J Ethnopharmacol*. 2001;75(2):77–87.
13. Ghasemi Pirbalouti A, Malekpoor F, Hamedi B. Ethnobotany and antimicrobial activity of medicinal plants of Bakhtiari Zagross mountains. *Iran J Med Plants Res*. 2012;6(5):675–679.
14. Rabbani M, Sajjadi SE, Sadeghi M. Chemical composition of the essential oil from *Kelussia odoratissima* Mozaff. and the evaluation of its sedative and anxiolytic effects in mice. *Clinics (Sao Paulo)*. 2011;66(5):843–848.
15. Ahmadi F, Kadivar M, Shahedi M. Antioxidant activity of *Kelussia odoratissima* Mozaff. in model and food systems. *Food Chem*. 2007;105(1):57–64.
16. Behbahani M. Evaluation of cytotoxic effect of *Kelussia odoratissima* Mozaff grown in Kohrang and Freydonshahr regions against MCF7 cell line and peripheral blood monolayer cell (PBMC). *Res Med*. 2015;38(4):221–225.
17. Khon VC, Mokhov I. Model estimates for the sensitivity of atmospheric centers of action to global climate changes. *Izvestiya Atmos Ocean Phys*. 2006;42(6):688–695.
18. Pirbalouti AG, Aghaee K, Kashi A, Malekpoor F. Chemical composition of the essential oil of wild and cultivated plant populations of *Kelussia odoratissima* Mozaff. *J Med Plant Res*. 2012;6(3):449–454.
19. Karimian H, Fadaeinasab M, Moghadamtousi SZ, et al. Chemopreventive activity of *Ferulago angulata* against breast tumor in rats and the apoptotic effect of polycerasoidin in MCF7 cells: a bioassay-guided approach. *PLoS One*. 2015;10(5):e0127434.
20. Karimian H, Fadaeinasab M, Moghadamtousi SZ, et al. The chemopreventive effect of *Tanacetum polycephalum* against LA7-induced breast cancer in rats and the apoptotic effect of a cytotoxic sesquiterpene lactone in MCF7 cells: a bioassay-guided approach. *Cell Physiol Biochem*. 2015;36(3):988–1003.
21. Logue SE, Elgendy M, Martin SJ. Expression, purification and use of recombinant annexin V for the detection of apoptotic cells. *Nat Protoc*. 2009;4(9):1383–1395.
22. Paydar M, Kamalidehghan B, Wong YL, Wong WF, Looi CY, Mustafa MR. Evaluation of cytotoxic and chemotherapeutic properties of boldine in breast cancer using in vitro and in vivo models. *Drug Des Devel Ther*. 2014;8:719.
23. Ali NM, Akhtar MN, Ky H, et al. Flavokawain derivative FLS induced G2/M arrest and apoptosis on breast cancer MCF-7 cell line. *Drug Des Devel Ther*. 2016;10:1897.
24. Fabisiak JP, Borisenko GG, Kagan VE. Quantitative method of measuring phosphatidylserine externalization during apoptosis using electron paramagnetic resonance (EPR) spectroscopy and annexin-conjugated iron. *Mol Toxicol Protocol*. 2014;1105:613–621.
25. Cragg GM, Newman DJ. Plants as a source of anti-cancer agents. *J Ethnopharmacol*. 2005;100(1):72–79.
26. Sajjadi SE, Shokoohinia Y, Moayedi N-S. Isolation and identification of ferulic acid from aerial parts of *Kelussia odoratissima* Mozaff. *Jundishapur J Nat Pharm Prod*. 2012;7(4):159.
27. Formigli L, Papucci L, Tani A, et al. Aponecrosis: morphological and biochemical exploration of a syncretic process of cell death sharing apoptosis and necrosis. *J Cell Physiol*. 2000;182(1):41–49.

28. Kim J-S, He L, Lemasters JJ. Mitochondrial permeability transition: a common pathway to necrosis and apoptosis. *Biochem Biophys Res Commun*. 2003;304(3):463–470.
29. Coqueret O. New roles for p21 and p27 cell-cycle inhibitors: a function for each cell compartment? *Trends Cell Biol*. 2003;13(2):65–70.
30. Esposito L, Indovina P, Magnotti F, Conti D, Giordano A. Anticancer therapeutic strategies based on CDK inhibitors. *Curr Pharm Des*. 2013; 19(30):5327–5332.
31. Arbab AS. Activation of alternative pathways of angiogenesis and involvement of stem cells following anti-angiogenesis treatment in glioma. *Histol Histopathol*. 2012;27(5):549.
32. Karimian H, Moghadamtousi SZ, Fadaeinasab M, et al. *Ferulago angulata* activates intrinsic pathway of apoptosis in MCF-7 cells associated with G1 cell cycle arrest via involvement of p21/p27. *Drug Des Devel Ther*. 2014;8:1481–1497.
33. Wu C-C, Bratton SB. Regulation of the intrinsic apoptosis pathway by reactive oxygen species. *Antioxid Redox Signal*. 2013;19(6):546–558.
34. Caroppi P, Sinibaldi F, Fiorucci L, Santucci R. Apoptosis and human diseases: mitochondrion damage and lethal role of released cytochrome C as proapoptotic protein. *Curr Med Chem*. 2009;16(31): 4058–4065.
35. Ng K-B, Bustamam A, Sukari MA, et al. Induction of selective cytotoxicity and apoptosis in human T4-lymphoblastoid cell line (CEMss) by boesenbergin a isolated from *Boesenbergia rotunda* rhizomes involves mitochondrial pathway, activation of caspase 3 and G2/M phase cell cycle arrest. *BMC Complement Altern Med*. 2013;13(1):41.
36. Green DR, Kroemer G. The pathophysiology of mitochondrial cell death. *Science*. 2004;305(5684):626–629.
37. Ola MS, Nawaz M, Ahsan H. Role of Bcl-2 family proteins and caspases in the regulation of apoptosis. *Mol Cell Biochem*. 2011;351(1–2): 41–58.